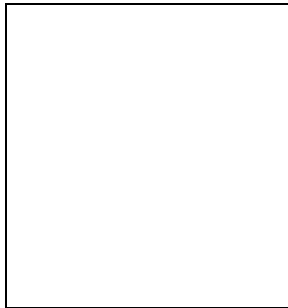


# THE CONTRIBUTION OF GALAXIES TO THE IR BACKGROUND

B. Guiderdoni <sup>1</sup>, E. Hivon <sup>2</sup>, & F.R. Bouchet <sup>1</sup>

<sup>1</sup> *Institut d'Astrophysique de Paris, CNRS, 98bis Boulevard Arago F-75014 Paris, France.*

<sup>2</sup> *Theoretical Astrophysics Center, Juliane Maries Vej 30, DK-2100 Copenhagen, Denmark.*



## Abstract

A new semi-analytic modelling of galaxy evolution in the IR/submm is hereafter outlined. This type of approach successfully reproduces the *optical* properties of galaxies. We illustrate a simple extension to the IR/submm wavelength range by taking the case of the SCDM model. We design a family of evolutionary scenarios with star formation histories reproducing the evolution of the overall gas and luminosity densities in the universe. These scenarios are also consistent with IRAS data and preliminary ISO counts, and we use them to disentangle the “Cosmic Infrared Background” detected by Puget *et al.* (1996) into discrete sources. We finally give predictions for the faint galaxy counts and redshift distributions in various submm wavelengths, which seem to be very sensitive to the details of the evolutionary scenarios. As a consequence, it is easy to anticipate that the current and forthcoming instruments, such as SCUBA, FIRST and PLANCK, will strongly constrain the evolution of high- $z$  galaxies.

## 1 Introduction

The epoch of galaxy formation can be observed by its imprint on the background radiation which is produced by the accumulation of the light of extragalactic sources along the line of sight. The search for the “Cosmic Optical Background” (hereafter COB) currently gives only upper limits. However, the shallowing of the faint counts obtained in the Hubble Deep Field (HDF, Williams *et al.* 1996) suggests that we are now close to convergence. Thus an estimate of the COB can be obtained by summing up the contributions of faint galaxies. At larger wavelengths, the DIRBE instrument on COBE has only given upper limits on the FIR background at 2 – 300  $\mu\text{m}$ , while Puget *et al.* (1996) have discovered an isotropic component in the COBE/FIRAS residuals between 200  $\mu\text{m}$  and 2 mm. We shall assume that this is the

long-sought ‘‘Cosmic Infrared Background’’ (hereafter CIB). Such a detection yields the first ‘‘post-IRAS’’ constraint on the evolution of high-redshift galaxies in the IR/submm range, before the era of ISO results. As shown in fig. 1, its level comparable to the estimate of the COB obtained by integrating the contributions of faint counts suggests that a significant fraction of the energy of young stars is absorbed by dust and released in the IR/submm.

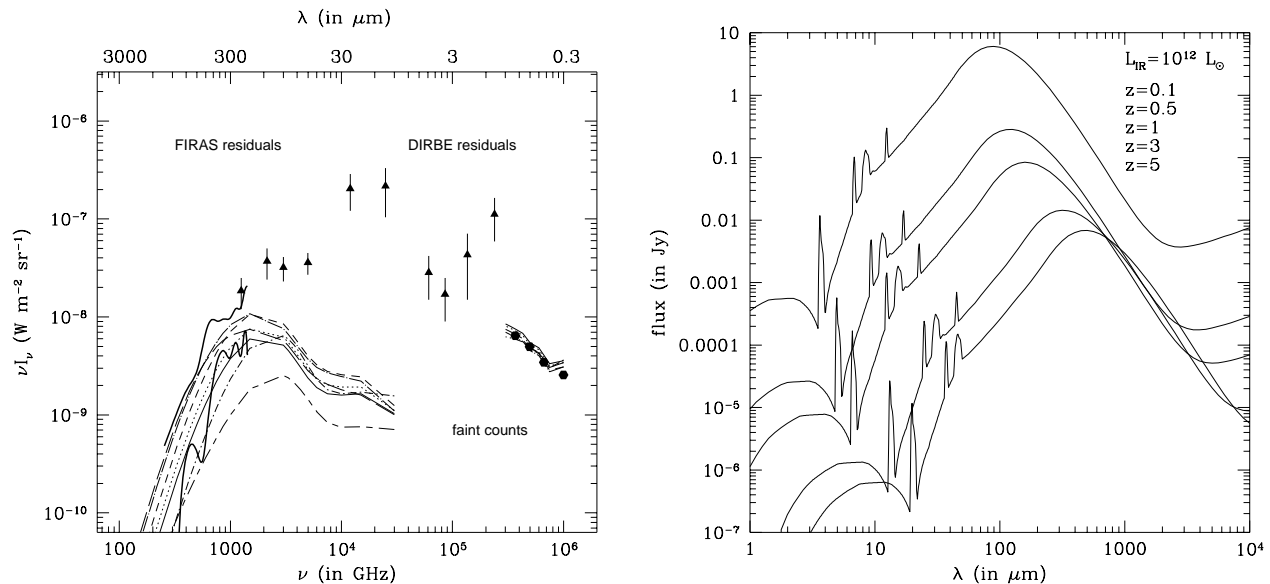


Figure 1: *Left-hand panel:* Predictions of the diffuse backgrounds in the IR/submm and in the optical compared to the current upper limits and detections. The solid triangles show the level of COBE/DIRBE residuals from Hauser (1995). The similar shapes of the residuals and dark sky suggest that the subtraction of foregrounds has been incomplete and that the plotted values are only upper limits. The thick solid lines give the CIB detection at  $\pm 1\sigma$  per point from the re-analysis of the COBE/FIRAS residuals, initiated in Puget *et al.* (1996) and revisited in Guiderdoni *et al.* (1997a). The solid hexagons show the Cosmic Optical Background (COB) obtained by summing up faint galaxy counts down to the Hubble Deep Field limit. The small dashes and long dashes give the prediction for no-evolution integrated up to redshift  $z_{for} = 8$  in a cosmology with  $h = 0.5$  and  $\Omega_0 = 1$ . The other curves are computed for the SCDM model with  $h = 0.5$ ,  $\Omega_0 = 1$ ,  $\sigma_8 = 0.67$ . The scenarios of tab. 1 are plotted with the following line codes: Q (dots and small dashes), A (solid line), B (dotted line), C (long dashes), D (short dashes), and E (dots and long dashes). Scenarios Q and A are not sufficient to fall within the acceptable range for the CIB. This suggest the existence of an additional population of ULIGs taken into account in scenarios B, C, D, and E. *Right-hand panel:* Observer-frame model spectra of a  $L_{IR} = 10^{12} L_{\odot}$  galaxy at increasing redshifts (from top to bottom). The reader is invited to note that the apparent flux in the submm range is almost insensitive to redshift, because the shift of the  $100 \mu\text{m}$  bump counterbalances the distance dimming.

At the moment, our understanding of galaxy evolution is mainly based on the recent breakthroughs brought by UV/visible observations (Lilly *et al.* 1995; Steidel *et al.* 1996; Williams *et al.* 1996). These results nicely match a scenario where star formation in bursts triggered by interaction/merging consumes the gas content of galaxies as time goes on. But the total amount of energy released by stars should be estimated by summing up the UV/visible light of stellar populations directly escaping from the galaxy, and the part which has been absorbed by dust and re-emitted in the IR/submm wavelength range. The corrections needed to account for dust extinction are rather uncertain and might induce an upward revision of the high-redshift star formation rates (SFR) deduced from UV/visible observations (Madau *et al.* 1996) by fac-

tors of a few. Moreover, a significant fraction of star formation might be completely hidden in heavily-extinguished galaxies which are missed by the above-mentioned observations. While we have learned from IRAS that about one third of the bolometric luminosity in the local universe is released in the IR/submm (Soifer and Neugebauer 1991), we know very little about galaxy evolution in this wavelength range. Faint galaxy counts and redshift surveys down to flux densities  $S_\nu \sim 60$  mJy (at  $60 \mu\text{m}$ ) do not probe deeper than  $z \sim 0.2$  (Ashby *et al.* 1996; Clements *et al.* 1996a). These surveys seem to show a strong luminosity and/or density evolution of IRAS sources, but it is difficult to extrapolate this trend to higher redshifts on a firm ground. It is expected that the ISO satellite will considerably complete and detail this picture. The ISO-HDF counts at  $15 \mu\text{m}$  show clear evidence of evolution (Oliver *et al.* 1997).

The so-called *semi-analytic* approach, which has been successfully applied to the prediction of the statistical properties of galaxies, includes the dissipative and non-dissipative processes ruling galaxy formation in dark matter haloes, complemented by star formation, stellar evolution and stellar feedback to the interstellar medium (White and Frenk 1991; Lacey and Silk 1991; Lacey *et al.* 1993, Kauffmann *et al.* 1993, 1994; Cole *et al.* 1994; Baugh *et al.* 1996, and other papers in these series). It turns out that, in spite of differences in the details of the models, these studies lead to conclusions in the UV, visible and (stellar) NIR which are remarkably similar. But none of these models has been applied so far to the prediction of the properties of galaxies in the IR/submm range. This is the main aim of this study which uses a simple version of the semi-analytic approach to disentangle the CIB into discrete units, and to give predictions of faint counts at wavelengths between  $60 \mu\text{m}$  and 1 mm. A detailed version of this work is presented in Guiderdoni *et al.* (1997a,b) and Hivon *et al.* 1997.

## 2 A brief outline of the semi-analytic approach

### 2.1 Non-dissipative and dissipative collapses

If we assume that the universe is dominated by non-baryonic dark matter, the formation and evolution of a galaxy in its dark matter halo can be briefly sketched as follows: the initial perturbation, which is gravitationally dominated by non-baryonic dark matter, grows and collapses. After the (non-dissipative) collapse, and subsequent violent relaxation, the halo virializes, through the formation of a mean potential well seen by all particles, which consequently share the same velocity distribution. The shock-heated baryonic component cools and collapses at the centre of the potential well. The baryons initially have the small rotation velocity of the halo created by tidal interactions with other haloes. Because of angular momentum conservation, their collapse stops when they reach rotational equilibrium.

### 2.2 Star formation and stellar feedback

Stars begin to form in this disk-like baryonic core and evolve through the main stages of stellar evolution. Observations seem to show that the SFR per unit surface density is proportional to the total gas surface density (neutral plus molecular) divided by the dynamical time scale of the disk (Kennicutt 1997). So we shall hereafter assume that the star formation rate is  $SFR(t) = M_{gas}(t)/t_\star$  with  $t_\star \equiv \beta t_{dyn}$ , the dynamical time scale of the disk. The free parameter  $\beta = 100$  accomodates the histogramme of “Roberts times” observed for a sample of 63 bright disk galaxies by Kennicutt *et al.* (1994). The Initial Mass Function is Salpeter’s. The spectrophotometric evolution, gas content and metallicity are consistently followed as in Guiderdoni and Rocca-Volmerange (1987), with upgraded stellar data.

The feedback can be local or non-local. Local feedback is due to supernova explosions and introduces a cut-off in the fraction of stars that form before the triggering of the galactic wind  $F_* = (1 + (V_{hot}/V_c)^\alpha)^{-1}$ . Cole *et al.* (1994) give the values  $V_{hot} = 130 \text{ km s}^{-1}$  and  $\alpha = 5$  from numerical simulations. Non-local feedback is due to reheating (Efstathiou 1992) at  $z \geq 2$  in haloes with  $V_c \leq V_{equ} \equiv 20 - 50 \text{ km}^{-1}$  and possibly as high as  $V_c \leq (200)^{1/3} V_{equ}$  in case of adiabatic collapse. We choose to model the two feedbacks by taking a somewhat arbitrary  $(1 + z)$  dependence  $V_{hot} = 40(1 + z_{coll}) \text{ km s}^{-1}$ .

### 2.3 Dust absorption and emission

Part of the energy released by stars is absorbed by dust and re-emitted in the IR and submm ranges. The derivation of the IR/submm spectrum is a three-step process: i) Computation of the optical thickness of the disks. We assume that the gas is distributed in an exponential disk with truncation radius  $r_g$  (computed from  $r_g/r_{25} = 1.6$ , Bosma 1981). As in Guiderdoni and Rocca-Volmerange (1987), the extinction curve depends on the gas metallicity  $Z_g(t)$  according to power-law interpolations based on the Solar Neighbourhood and the Magellanic Clouds. ii) Computation of the amount of bolometric energy absorbed by dust. We assume a simple geometric distribution where the gas and the stars which contribute mainly to dust heating are distributed with equal scale heights in the disks (the so-called ‘‘slab’’ geometry). We average over inclination angle  $i$  and crudely take into account the effect of the albedo  $\omega_\lambda$  for isotropic scattering (Natta and Panagia 1984). iii) Computation of the spectral energy distribution of dust emission. The emission spectra are computed as a sum of various components, according to the method developed by Maffei (1994), from the observational correlations of the IRAS flux ratios  $12\mu\text{m}/60\mu\text{m}$ ,  $25\mu\text{m}/60\mu\text{m}$  and  $100\mu\text{m}/60\mu\text{m}$  with  $L_{IR}$  (Soifer and Neugebauer 1991). These correlations are extended to low  $L_{IR}$  with the sample of Rice *et al.* (1988). Several components are considered in the model spectra (according to Désert *et al.* 1990): Polycyclic aromatic hydrocarbons (PAH), very small grains (VSG) and big grains (BG). Synchrotron radiation is strongly correlated with the IR luminosity (see e.g. Helou *et al.* 1985). We extrapolate its contribution from 21 cm down to  $\sim 1 \text{ mm}$  with a single average slope 0.7.

Fig. 1 shows observer-frame *model* spectra of a luminous IR galaxy at various redshifts. It turns out that there is a wavelength range, between  $\sim 600 \mu\text{m}$  and  $\sim 4 \text{ mm}$ , where the distance effect is counterbalanced by the ‘‘negative k-correction’’ due to the huge rest-frame emission bump at  $\sim 100 \mu\text{m}$ . In this range, the apparent flux of galaxies depends weakly on redshift. The modelling of the observer-frame submm fluxes, faint galaxy counts and diffuse background of unresolved galaxies is consequently very sensitive to the early stages of galaxy evolution.

## 3 The history of star formation

### 3.1 Two modes of star formation

Hereafter, we consider the SCDM model with  $H_0 = 50 \text{ km s}^{-1} \text{ Mpc}^{-1}$ ,  $\Omega_0 = 1$ ,  $\Lambda = 0$ ,  $\sigma_8 = 0.67$ , and  $\Omega_{bar} = 0.05$  as an illustrative case. We need to introduce scenarios of evolution which will be used to compute the IR/submm properties of galaxies and to predict the CIB and faint galaxy counts. While a complete assessment of the energy budget of galaxies would require the monitoring of the multi-wavelength luminosity functions and galaxy counts (delayed to forthcoming studies), we hereafter only wish to address the issue of the overall evolution of the comoving gas (and SFR) density in the universe.

Fig. 2 shows the predicted gas evolution for scenario Q with  $\beta = 100$ . It corresponds to the fit of SFR timescales in disks, that is, the so-called “Roberts times” peaking at 3 Gyr and ranging between 0.3 and 30 Gyr (Kennicutt *et al.* 1994). Clearly the gas density does not decline fast enough between  $z = 1$  and the local universe because the SFR is not high enough. It is not surprising to check in fig. 1 that the predicted background is below the acceptable range for the CIB.

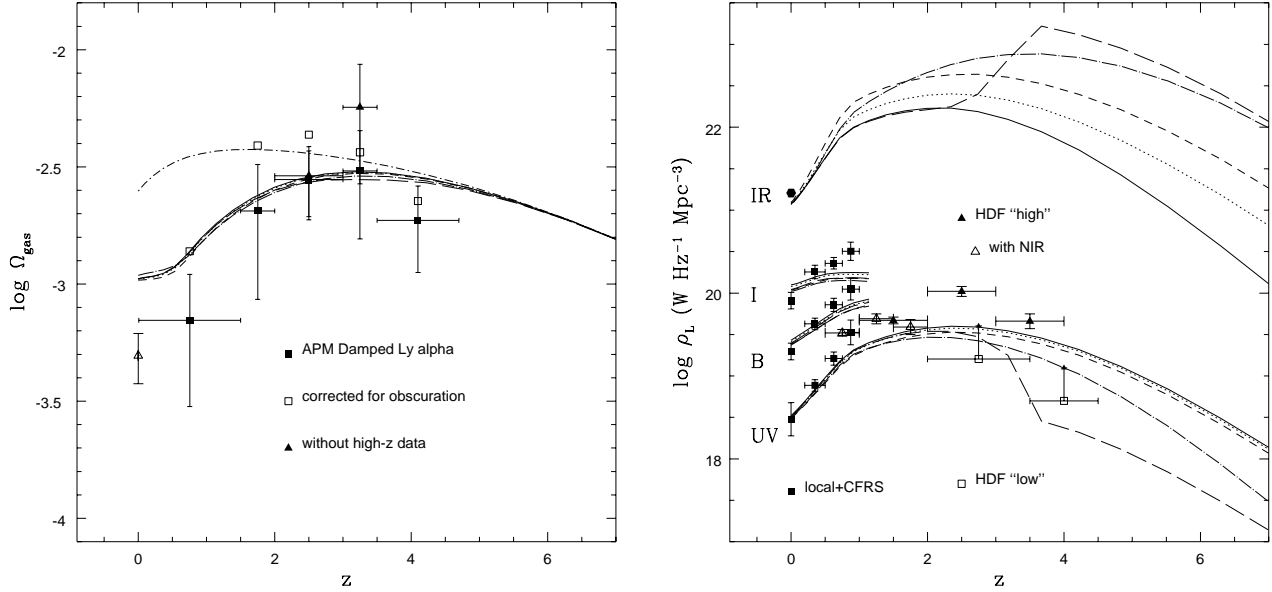


Figure 2: *Left-hand panel:* Evolution of the cold gas density parameter in damped Lyman- $\alpha$  systems. Solid triangles: data without the APM QSO survey. Solid squares: data including the APM QSO survey. Open squares: tentative correction for selection effects due to QSO obscuration (Storrie-Lombardi *et al.* 1996). Open triangle: local estimate from HI surveys (Briggs and Rao 1993). Scenario Q (“quiet” mode,  $\beta = 100$ ) is plotted with dots and small dashes. Other scenarios (plotted with line codes of fig. 1) involve a “burst” mode ( $\beta = 10$ ) fraction increasing with redshift. The various scenarios involving the “burst” mode consume more gas than the “quiet” mode. *Right-hand panel:* Rest-frame comoving luminosity densities. Letters UV, B, I and IR respectively stand for 2800Å, 4400 Å, 10000 Å and 60  $\mu\text{m}$ . The emissivity at 1600 Å is about 30 % higher than at 2800 Å. Solid squares: local and Canada-France Redshift Survey (Lilly *et al.* 1996). Open triangles: NIR data are taken into account to compute photometric redshifts in the Hubble Deep Field (Connolly *et al.* 1997). Solid triangles: other estimates of photometric redshifts in the HDF (Sawicki *et al.* 1997). Open squares: HDF with redshifts from Lyman-continuum drop-outs (Madau *et al.* 1996). Solid hexagon: 60  $\mu\text{m}$  local density corresponding to one third of the bolometric light radiated in the IR (Saunders *et al.* 1990). Scenario A (solid line) has no ULIGs. Various quantities of ULIGs are included in scenarios B (dotted line), C (long dashes), D (short dashes), and E (dots and long dashes). See tab. 1 for details. The different UV and IR emissions mainly result from different IMF and extinction, with almost similar SFR histories, and they are not strongly constrained by the current status of (possibly discrepant) UV/visible observations.

We now consider a mix of two broad types of populations, one with a “quiet” star formation rate, the other proceeding in bursts with  $\beta = 10$ . For the “burst” mode, we take an involved mass fraction increasing with collapse redshift  $f_{\text{burst}}(z) = f_{\text{burst}}(0)(1 + z_{\text{coll}})^\gamma$ , as suggested by the increasing fraction of blue objects showing tidal and merger features at larger  $z$  (Abraham *et al.* 1996). Noting that the frequency of galaxy pairs is  $\propto (1 + z)^\delta$  with  $\delta$  ranging between 2 and 6 at  $\pm 1\sigma$  (Zepf and Koo 1989; Burkey *et al.* 1994; Carlberg *et al.* 1994), we choose here a

high evolution rate  $\gamma = 5$ . Then  $f_{burst}(0)$  is set to 0.04 in order to fit the SFR density at low  $z$ , resulting in an “all–burst” behaviour at  $z \geq 0.8$ . This will be our scenario A. As shown in fig. 2, this phenomenological description of the increasing importance of the bursts reproduces the steep decline of the gas density. The origin of this fast evolution has still to be elucidated by a more exhaustive modelling of all interaction processes in semi–analytic codes following the merging history trees of haloes and galaxies.

We can now compute the corresponding IR/submm emission by taking the conservative estimate of the average optical thickness and “slab” geometry as in the “quiet” mode. As a result, this population of “mild starbursts” and “luminous UV/IR galaxies” (LIGs) has IR–to–blue luminosity ratios in the range  $0.06 \leq L_{IR}/\lambda_B L_B \leq 4$  which is characteristic of blue–band selected samples (Soifer *et al.* 1987), and should be fitted to the Canada–France Redshift Survey (CFRS, selected in the observer–frame  $I_{AB}$  band, roughly corresponding to the  $B$  band at  $z \sim 1$ ), and to high– $z$  HDF galaxies. The evolution of the comoving luminosity density in various UV/visible bands and at  $60 \mu\text{m}$  is compared to observational estimates in fig. 2. The local energy budget and its evolution from  $z = 0$  to 1 seem to be fairly reproduced. As shown in fig. 1, scenario A reproduces the COB, and gives a predicted IR/submm background which is clearly barely compatible with the observed CIB whose mean amplitude is twice the prediction, despite our high choice of  $\gamma$ . Consequently, we can easily suspect the existence of a population of galaxies which are more heavily extinguished.

Table 1: Scenarios of galaxy evolution

Name	$f_{burst}$ ( $\beta = 10$ )	$f_{quiet}$ ( $\beta = 100$ )	% of ULIGs
Q	0	1	0 %
A	$0.04(1 + z_{coll})^5$	$1 - f_{burst}$	0 %
B	$0.04(1 + z_{coll})^5$	$1 - f_{burst}$	5 % at all $z$
C	$0.04(1 + z_{coll})^5$	$1 - f_{burst}$	90 % for $z_{coll} > 3.5$
D	$0.04(1 + z_{coll})^5$	$1 - f_{burst}$	15 % at all $z$
E	$0.04(1 + z_{coll})^5$	$1 - f_{burst}$	$1 - \exp -0.02(1 + z_{coll})^2$

### 3.2 A heavily–extinguished component

The above–mentioned CIB computed with scenario A seems to be sort of a conservative estimate of the minimum IR/submm background due to typical CFRS and HDF galaxies. We now wish to assess how much star formation might be hidden by dust shrouds and introduce an additional population of heavily–extinguished bursts, which are similar to “ultra–luminous IR galaxies”, or ULIGs (Sanders and Mirabel 1996; Clements *et al.* 1996a,b). We maximize their IR luminosity by assuming that all the energy available from stellar nucleosynthesis ( $0.007xMc^2$ ) is radiated in a heavily–extinguished medium. We take  $\langle x \rangle = 0.40$  for stars with masses larger than  $\sim 5M_\odot$ . We distribute this population of ULIGs in two ways: i) A constant mass fraction of 5 % (scenario B) or 15 % (scenario D) at all  $z$ , mimicking a scenario of continous bulge formation as the end–product of interaction and merging. ii) 90 % of all galaxies forming at high  $z_{coll} \geq 3.5$  undergo a heavily–extinguished burst, mimicking a strong episode of bulge formation. These scenarios are now able to fit both the COB and CIB as shown in fig. 1. Scenarios B and D seem more appropriate to reproducing the CIB at  $300 \mu\text{m}$  while scenario C, with high– $z$  ULIGs, has a stronger contribution at larger wavelengths. Of

course, these last three cases are only illustrative, and a combination of these solutions would also fit the CIB. For instance, we introduce an ad hoc scenario E with a fraction of ULIGs increasing as  $1 - \exp -0.02(1 + z_{coll})^2$ . Such a dependence can be obtained if the fraction of ULIGs depends on the mean surface density and optical thickness of disks which roughly scale as  $(1 + z_{coll})^2$  in our modelling. Scenario E nicely fits the COB and CIB.

It is clear from fig. 2 that none of the optical data reflects the large differences between these scenarios, although the fraction of light in the IR varies widely at high  $z$ . In scenario A, the IR/UV ratio decreases with increasing  $z$  because of the decreasing metallicity of galaxies. In scenario B and D, this effect is cancelled because the ULIG bursts are assumed to be optically-thick, and the IR/UV ratio at  $z = 4$  is similar to that at  $z = 0$ . In scenario C and E, the IR/UV ratio strongly increases with  $z$  and is  $\sim 100$  times higher than for model B at  $z = 4$ . One should note that at this redshift, scenario C and E are roughly consistent with the lower limits of the UV-luminosity density derived from Lyman-continuum drop-outs, but with ten times as much SFR as directly derived if extinction is not taken into account. In these scenarios, galaxy formation at high  $z$  is an almost completely-obscured process.

## 4 Predictions of FIR and submm counts

Fig. 3 gives the predictions for the IRAS 60  $\mu\text{m}$  differential counts normalised to the Euclidean slope. All the scenarios involving an increasing fraction of the “burst” mode predict more galaxies than the no-evolution curve. Scenario D with 15 % of ULIGs is rejected by the data. All the other scenarios have a moderate local fraction of ULIGs and are in agreement with the faint counts. Scenario E with an increasing fraction of ULIGs gives an almost flat curve which is reminiscent of the observational trend. Fig. 3 also gives predicted faint counts at 15  $\mu\text{m}$  (compared with the ISO-HDF, Oliver *et al.* 1997) and at 175  $\mu\text{m}$  (compared with preliminary ISOPHOT counts, Kawara *et al.* 1997). Guiderdoni *et al.* (1997a) emphasized the relative degeneracy of the predictions at wavelengths shorter than 100  $\mu\text{m}$ , including the IRAS 60  $\mu\text{m}$  and ISOCAM 15  $\mu\text{m}$  counts, and the strong sensitivity of the submm counts to the details of galaxy evolution. While the IRAS data do not yield tight constraints on the evolution of galaxies at  $z \geq 0.2$ , the on-going deep surveys with ISO and the forthcoming ones with SCUBA in the atmospheric windows at 450 and 850  $\mu\text{m}$  (for which the array is matched to the instrument optics) will quickly help discriminate between the various scenarios, in the expectation of PLANCK and FIRST. The 10 mJy level which will be reachable by the forthcoming submm observations with SCUBA and FIRST will allow the surveys to begin “breaking” the CIB into discrete units. As shown in fig. 3, a large fraction of these objects are at redshifts beyond 1.

## 5 Conclusions

Predictions of IR/submm galaxy counts, redshift distributions, and diffuse background of unresolved galaxies can be obtained from a semi-analytic model of galaxy formation and evolution which takes into account the main physical processes from the collapse of the density fluctuations to the absorption of UV and visible star light by dust and the re-emission at larger wavelengths. This new model is consistent with the dynamical process of continuous galaxy formation predicted by the hierarchical growth of structures in a SCDM universe, and represents a significant progress with respect to previous phenomenological models designed to make predictions in the IR/submm.

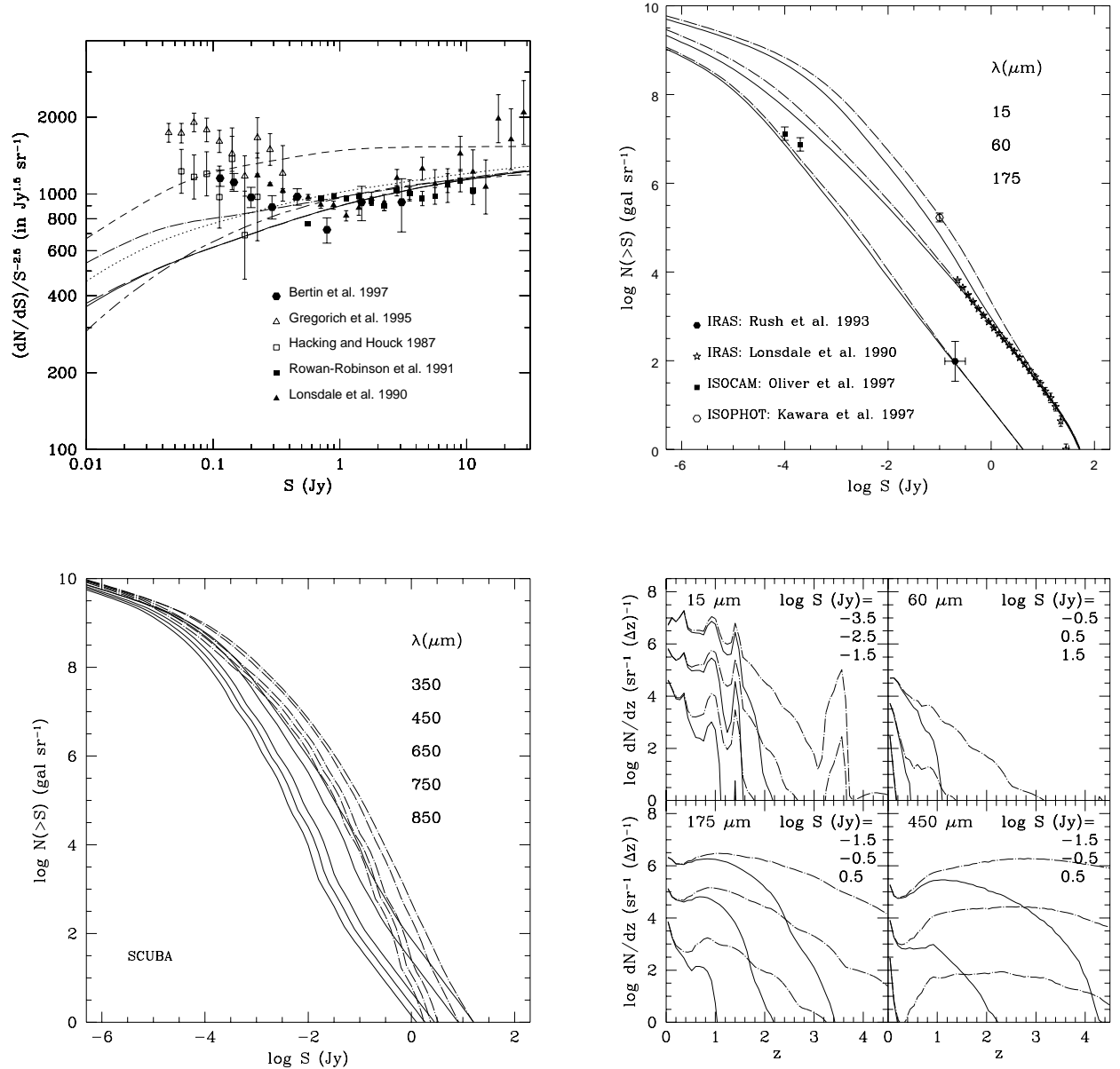


Figure 3: *Left-hand, top panel:* Predictions for differential galaxy counts (normalised to Euclidean counts) at  $60\ \mu\text{m}$ . Data is shown for IRAS counts. Open stars: Faint Source Survey (Lonsdale *et al.* 1990). Open squares: QMW survey (Rowan–Robinson *et al.* 1991). Solid squares: North Ecliptic Pole Region (Hacking and Houck 1987). These latter counts might be affected by the presence of a supercluster. Solid hexagons: Very Faint Source Survey (Bertin *et al.* 1997). The counts by Gregorich *et al.* (1995), which are plotted with open triangles, are contaminated by cirrus. The no-evolution model (for a cosmology with  $h = 0.5$ ,  $\Omega_0 = 1$ ) is shown with the short and long dashes. Scenarios A, B, C, D, E are plotted with line codes as in fig. 1. *Right-hand, top panel:* Predictions for faint counts at  $15\ \mu\text{m}$ ,  $60\ \mu\text{m}$  and  $175\ \mu\text{m}$  (from bottom to top) for scenarios A and E. Note that the  $15\ \mu\text{m}$  fluxes only include dust emission, and are lower limits for  $z \geq 1$ . Open stars: Faint Source Survey (Lonsdale *et al.* 1990). Solid hexagon: Rush *et al.* 1993. Solid squares: ISO–HDF (Oliver *et al.* 1997) with ISOCAM at  $15\ \mu\text{m}$ . Open hexagon: preliminary counts by Kawara *et al.* (1997) with ISOPHOT at  $175\ \mu\text{m}$ . *Left-hand, bottom panel:* Predictions at SCUBA wavelengths for scenarios A and E. In contrast with counts at wavelengths smaller than  $100\ \mu\text{m}$ , the submm counts are very sensitive to the details of the high- $z$  evolution, because of the shift of the  $100\ \mu\text{m}$  bump into the observing bands. *Right-hand, bottom panel:* Predictions of redshift distributions in various bands for scenarios A and E. The central values of the  $\Delta \log S_\nu = 1$  flux bins (in Jy) are indicated from top to bottom.



While the cosmological context and the rules of dissipative collapse are fixed, there is some freedom in the choice of the evolutionary scenarios, through a series of free parameters describing star formation ( $\beta$ ) and feedback ( $\alpha$  and  $V_{hot}$ ). In this first study, we chose to accommodate a selected set of data: the comoving SFR, gas and UV/visible luminosity densities. Since the “quiet” mode of star formation ( $\beta = 100$ ) is unable to reproduce the data, we have to introduce a mass fraction involved in the “burst” mode ( $\beta = 10$ ) increasing with redshift as  $(1 + z_{coll})^5$  and likely associated to the increasing rate of interaction and merging. This phenomenological ansatz allows the scenarios to reproduce the evolution of the overall properties of galaxies between  $z = 1$  and 0, and has yet to be explained.

Then we compute the IR properties of these galaxies. In order to reproduce both the COB and CIB, it is necessary to introduce an additional population of heavily-extinguished sources. We design several scenarios consistent with the CIB and our selected set of data. The IRAS 60  $\mu\text{m}$  counts are only sensitive to low- $z$  galaxies and weakly constrain these scenarios, though they seem to limit the fraction of local ULIGs. On the contrary, the ISOCAM counts at 15  $\mu\text{m}$ , and especially the ISOPHOT and other submm counts are sensitive to the details of the evolutionary scenarios. The on-going observations with ISO should already discriminate between the range of possibilities which are still consistent with the IRAS data. Future observations with SCUBA and FIRST at the 10 mJy level will help put strong constraints on the evolution at  $z \geq 1$ , and begin to “break” the CIB into discrete sources.

## References

- [1] Abraham, R.G., Tanvir, N.R., Santiago, B.X., Ellis, R.S., Glazebrook, K., van den Bergh, S., 1996, MNRAS, 279, L47
- [2] Ashby, M.L.N., Hacking, P.B., Houck, J.R., Soifer, B.T., Weisstein, E.W., 1996, ApJ, 456, 428
- [3] Baugh, C.M., Cole, S., Frenk, C.S., 1996b, MNRAS, 283, 1361
- [4] Bosma, A., 1981, AJ, 86, 1825
- [5] Briggs, F.H., Rao, S., 1993., ApJ 417, 494
- [6] Burkey, J.M., Keel, W.C., Windhorst, R.A., Franklin, B.E., 1994, ApJ, 429, L13
- [7] Carlberg, R.G., Pritchet, C.J., Infante, L., 1994, ApJ, 435, 540
- [8] Clements, D.L., Sutherland, W.J., Saunders, W., Efstathiou, G.P., McMahon R.G., Maddox, S., Rowan–Robinson, M., 1996a, MNRAS, 279, 459
- [9] Clements, D.L., Sutherland, W.J., McMahon R.G., Saunders, W., 1996b, MNRAS, 279, 477
- [10] Cole, S., Aragón–Salamanca, A., Frenk, C.S., Navarro, J.F., Zepf, S.E. 1994., MNRAS, 271, 781
- [11] Connolly, A.J., Szalay, A.S., Dickinson, M., SubbaRao, M.U., Brunner, R.J., 1997, astro-ph/9706255
- [12] Désert, F.X., Boulanger, F., Puget, J.L. 1990, A&A, 237, 215
- [13] Efstathiou, G., 1992, MNRAS, 256, 43P
- [14] Gregorich, D.T., Neugebauer, G., Soifer, B.T., Gunn, J.E., Herter, T.L., 1995, AJ, 110, 259
- [15] Guiderdoni, B., Rocca–Volmerange, B. 1987, A&A, 186, 1
- [16] Guiderdoni, B., Bouchet, F.R., Puget, J.L., Lagache, G., Hivon, E., 1997a, *submitted*

- [17] Guiderdoni, B., Hivon, E., Bouchet, F.R., Maffei, B., 1997b, *submitted*
- [18] Hacking, P., Houck, J.R., 1987, *ApJSS*, 63, 311
- [19] Hauser, M.G. 1995, in *Proceedings of the IAU Symp. n° 168, Examining the Big Bang and Diffuse Background Radiation*, The Hague, August 1994
- [20] Helou, G., Soifer, B.T., Rowan–Robinson, M., 1985, *ApJ*, 298, L7
- [21] Hivon, E., Guiderdoni, B., Bouchet, F., *in preparation*
- [22] Kauffmann, G.A.M., White, S.D.M., Guiderdoni, B., 1993, *MNRAS*, 264, 201
- [23] Kauffmann, G.A.M., Guiderdoni, B., White, S.D.M., 1994, *MNRAS*, 267, 981
- [24] Kawara, K., Taniguchi, Y., Sato, Y., Okuda, H., Matsumoto, T., *et al.*, 1997, *ESA FIRST Symposium*
- [25] Kennicutt, R.C., 1997, in *Starbursts: Triggers, Nature and Evolution*, B. Guiderdoni and A. Kembhavi (eds.), Editions de Physique /Springer–Verlag
- [26] Kennicutt, R.C., Tamblyn, P., Congdon, C.W., 1994, *ApJ*, 435, 22
- [27] Lacey, C., Silk, J., 1991, *ApJ*, 381, 14
- [28] Lacey, C., Guiderdoni, B., Rocca–Volmerange, B., Silk, J., 1993, *ApJ*, 402, 15
- [29] Lilly, S.J., Tresse, L., Hammer, F., Crampton, D., Le Fèvre, O., 1995, *ApJ*, 455, 108
- [30] Lilly, S.J., Le Fèvre, O., Hammer, F., Crampton, D., 1996, *ApJ*, 460, L1
- [31] Lonsdale, C.J., Hacking, P.B., Conrow, T.P., Rowan–Robinson, M., 1990, *ApJ*, 358, 60
- [32] Madau, P., Ferguson, H.C., Dickinson, M.E., Giavalisco, M., Steidel, C.C., Fruchter, A., 1996, *MNRAS*, 283, 1388
- [33] Maffei, B. 1994, PhD Dissertation, Université Paris VII
- [34] Natta, A., Panagia, N., 1984, *ApJ*, 287, 228
- [35] Oliver, S.J., Goldschmidt, P., Franceschini, A., Serjeant, S.B.G., Efstathiou, A.N., *et al.*, 1997, *astro-ph/9707029*
- [36] Puget, J.L., Abergel, A., Boulanger, F., Bernard, J.P., Burton, W.B., *et al.*, 1996, *A&A*, 308, L5
- [37] Rice, W., Lonsdale, C.J., Soifer, B.T., Neugebauer, G., Kopan, E.L., Lloyd, L.A., de Jong, T., Habing, H.J., 1988, *ApJSS*, 68, 91
- [38] Rowan–Robinson, M., Saunders, W., Lawrence, A., Leech, K., 1991, *MNRAS*, 253, 485
- [39] Rush, B., Malkan, M.A., Spinoglio, L., 1993, *ApJSS*, 89, 1
- [40] Sanders, D.B., Mirabel, I.F., 1996, *ARAA*, 34, 749
- [41] Saunders, W., Rowan–Robinson, M., Lawrence, A., Efstathiou, G., Kaiser, N., Ellis, R.S., Frenk, C.S., 1990, *MNRAS*, 242, 318
- [42] Sawicki, M.J., Lin, H., Yee, H.K.C., 1997, *AJ*, 113, 1
- [43] Soifer, B.T., Sanders, D.B., Madore, B.F., Neugebauer, G., Danielson, G.E., *et al.*, 1987, *ApJ*, 320, 238
- [44] Soifer, B.T., Neugebauer, G., 1991, *AJ*, 101, 354
- [45] Steidel, C.C., Giavalisco, M., Pettini, M., Dickinson, M., Adelberger, K.L., 1996, *ApJ*, 462, L17
- [46] Storrie–Lombardi, L.J., McMahon, R.G., Irwin, M.J., 1996, *MNRAS*, 283, L79
- [47] White, S.D.M., Frenk, C.S., 1991, *ApJ*, 379, 52
- [48] Williams, R.E., *et al.*, 1996, *AJ*, 112, 1335
- [49] Zepf, S.E., Koo, D.C., 1989, *ApJ*, 337, 34